

Supporting Information for:

**Isolated, Well-Defined Organovanadium(III) on Silica: Single-Site
Catalyst for Hydrogenation of Alkenes and Alkynes**

H. Sohn,^a J. Camacho-Bunquin,^{a,*} R. R. Langeslay,^a P. A. Ignacio-de Leon,^b J. Niklas,^a O. G. Poluektov,^a C. Liu,^a J. G. Connell,^c D. Yang,^a J. Kropf,^a H. Kim,^{a,d} P. Stair,^{a,d} M. Ferrandon^a and M. Delferro^{a,*}

^aChemical Sciences and Engineering Division, ^bEnergy Systems Division, ^cMaterials Science Division, Argonne National Laboratory, 9700 S. Cass Ave., Lemont, IL 60439 USA. ^dCenter for Catalysis and Surface Science and Department of Chemistry, Northwestern University, Evanston, IL 60208, USA

E-mail: bunquin@anl.gov and delferro@anl.gov

Table of Contents:

1. Experimental Section	S2
1.1 Materials and methods	S2
1.2 Physical and analytical measurements	S2
1.3 DFT calculations	S4
1.4 X-ray absorption spectroscopy (XAS) measurements and analysis	S4
1.5 High-Throughput Catalysis Screening	S5
1.5.1 GC-MS and GC-FID Analysis	S6
1.5.2 Catalyst Recyclability and Leaching Tests	S6
1.6 Micro-reactor Activity Testing	S7
2. Results and discussion	S7
2.1 Synthesis of [(SiO ₂)V(Mes)(THF)] (1a-c)	S7
2.2 Synthesis of V ₂ O ₅ /SiO ₂	S8
2.3 Synthesis of [(SiO ₂)V(Mes)(THF)]-2,2'-bipyridine derivatives (2a-c)	S8
2.4 NMR-scale vanadation of SiO ₂ with [V(Mes) ₃ (THF)]	S8
2.5 TGA-MS results	S10
2.6 EPR results	S11
2.7 XPS analysis results	S13
2.8 DRUV-Vis spectroscopy	S14
2.9 DFT calculations	S16
2.10 SPR catalyst testing and catalyst recyclability results	S17
2.11 TEM imaging	S18
2.12 UV Raman results	S19
2.13 Variable-temperature gas-phase hydrogenation of ethylene	S20
3. References	S21

1. Experimental Section

1.1 Materials and Methods

Unless otherwise stated, all manipulations described below were carried out with rigorous exclusion of O₂ and moisture in oven-dried glassware in a N₂-filled MBraun glovebox with a high-capacity recirculator (<1 ppm O₂). Benzene-d₆ (Sigma-Aldrich) was dried over 4 Å molecular sieves and degassed using three freeze-pump-thaw cycles prior to use. Solvents were purchased from Sigma-Aldrich and were sparged with nitrogen and dried over activated alumina. The 1,3,5-tritertbutyl benzene internal integration standard for grafting NMR studies was purchased from Sigma-Aldrich, sublimed under high-vacuum, and stored in the glove box. Diphenylacetylene were purified by sublimation under high vacuum and were stored in a glovebox. The [V(Mes)₃(THF)] complex was prepared as reported in the literature.^{S1} Silica (high-purity, 35-60 mesh, pore size 150 Å, BET surface area 300 m²/g) was purchased from Sigma-Aldrich and activated at 200 °C under vacuum for 12 hours.

1.2 Physical and Analytical Measurements

Solution NMR experiments were conducted using a Bruker UltraShield 500 MHz spectrometer (¹H = 500 MHz, ¹³C = 125 MHz) and the spectra were analyzed using MNova (v111, Mestrelab Research S.L, Spain). Chemical shifts for ¹H spectra were referenced using internal solvent resonances and are reported relative to tetramethylsilane (TMS). Elemental analysis (V, C, H) was conducted by Galbraith Laboratories, Inc. (Knoxville, TN). Thermogravimetric analysis (TGA) was performed on a TA Instruments Discovery TGA equipped with a Stanford Research Systems QMS200 gas analyzer (MS). Samples were run under a nitrogen flow (5 mL/min) with a heating rate of 20 °C/min. Diffuse Reflectance Infrared Fourier Transform Spectroscopy (DRIFTS) spectra were acquired using Thermo Scientific™ Nicolet iS50 FT-IR Spectrometer equipped with an iS50 Automated Beamsplitter exchanger (ABX). The Praying Mantis™ accessory was used in order to collect the spectra of the samples under air-free and moisture-free conditions. The samples were prepared inside the glove box and placed on the sample cup of the high temperature reaction chamber which includes ZnSe windows. The reaction chamber was then sealed and transferred to the FT-IR spectrometer. The measurements were made using a MCT/A detector without flowing any gases through the reaction chamber. Dried KBr spectrum was used as a background.

Continuous-wave (CW) X-band (9-10 GHz) EPR experiments were carried out with a Bruker ELEXSYS II E500 EPR spectrometer (Bruker Biospin, Rheinstetten, Germany), equipped with a TE₁₀₂ rectangular EPR resonator (Bruker ER 4102ST). Quantitative characterization of the spin concentration was done using a pentahydrate CuSO₄ as reference sample. Data processing was done using Xepr (Bruker BioSpin, Rheinstetten) and Matlab 7.11.1 (The MathWorks, Inc., Natick) environment. A JEOL JEM-2100F transmission electron microscope (TEM) was used for all bright field imaging at 200 kV. Samples were prepared by dispersing solids in ethanol via sonication for 30 s. Colloidal suspensions were drop cast onto lacey C on Cu grids (300 mesh) from Electron Microscopy Sciences. The UV-Vis spectra were obtained by implementing UV-Vis-NIR spectrophotometer (Shimadzu UV-3600 Plus) including a PMT (photomultiplier tube) detector. Similar to DRIFTS experiment, sample preparation was conducted inside the glove box. The sample was first tightly packed in the sample cup of the Praying Mantis™ reaction cell and transferred to the spectrophotometer. The reflectance from the sample was measured from 200 to 700 nm at a medium scan speed with a sampling interval of 1 nm and a slit width of 8 nm. A background spectrum was obtained using polytetrafluoroethylene (PTFE) and was subtracted from the sample spectrum. Kubelka-Munk (K-M) and Tauc functions were plotted in order to obtain the band gap energies of the samples. The excitation wavelength of 375 nm for UV Raman measurements is provided by second-harmonic generation output of a 4 kHz repetition rate, nanosecond pulsed, wavelength-tunable Ti:Sapphire laser (Coherent, Indigo-S).^{S2} The laser power delivered to the catalyst was 1.7 mW. Raman spectra were recorded with a triple-grating spectrometer (Princeton Instruments, Trivista 555) equipped with a liquid N₂-cooled, UV-enhanced CCD detector. Prior to the measurements, samples were exposed to ambient air at room temperature. Then, UV Raman spectra were collected at room temperature with flowing He in the fluidized bed reactor described previously.^{S2} XPS measurements were performed using a Specs PHOIBOS 150 hemispherical energy analyzer using a monochromatic Al K α X-ray source. Powder samples were supported on carbon tape to enable introduction to UHV. The load-lock of the analytical UHV system is connected directly to an Ar atmosphere glovebox (O₂ and H₂O < 0.5 ppm), enabling loading of samples without any exposure to ambient atmosphere. Core level spectra were measured using a pass energy of 20 eV at a resolution of 0.05 eV/step and a total integration time of 0.5 sec/point. Deconvolution was performed using CasaXPS software with a Shirley-type

background and 70-30 Gaussian-Lorentzian peak shapes. Peaks were charge referenced using the position of the adventitious carbon 1s peak at 284.8 eV.

1.3 DFT Calculations

Density functional theory (DFT) calculations were carried out to investigate the local structure of the V^{3+} site on SiO_2 . A periodic model of SiO_2 was used based on our previous development.^{S3} The optimization of the structure was carried out using GGA_PBE method implemented in the Vienna Ab initio Simulation Package (VASP).^{S4-7} The $3 \times 3 \times 1$ k-points and a 400 eV energy cutoff were used. The UV-vis spectra of the V^{3+} site was calculated using a the cluster model of SiO_2 , in which the geometries of V and the ligands, as well as the Si and O of the SiO_2 backbone were taken from the periodic calculation, and the terminal Si were terminated with hydroxyl groups. The calculation of the spectra was carried out using CAM-B3LYP/6-31++G(d,p) level of theory implemented in Gaussian09 program package.^{S8}

1.4 X-ray Absorption Spectroscopy Measurements and Analysis

XAS experiments X-ray absorption measurements were acquired on the bending magnet beam line of the Materials Research Collaborative Access Team (MRCAT) at the Advanced Photon Source, Argonne National Laboratory. The data were collected in transmission step scan mode. Photon energies were selected using a water-cooled, double-crystal Si(111) monochromator, which was detuned by approximately 50% to reduce harmonic reflections. For V, the ionization chambers were optimized for the maximum current with linear response (~ 1010 photons detected/sec) with 10% absorption (25% N_2 and 75% He) in the incident ion chamber and 70% absorption (93% N_2 and 7% Ar) in the transmission detector. A V foil spectrum (edge energy 5465 eV) was acquired simultaneously with each measurement for energy calibration. All XAS samples were handled and prepared in a glovebox. Each solid standard sample was mixed with boron nitride to achieve a final weight ratio of about 2% with V. The mixture was mixed well with a mortar and pestle, and then 5-7 mg of the mixture was pressed into a cylindrical sample holder consisting of six wells with a radius of 2.0 mm, forming a self-supporting wafer. The sample holder was placed in a quartz tube (1 in. OD, 10 in. length) sealed with Kapton windows by two Ultra-Torr fittings and then used for transmission mode measurement. The edge energy of the X-Ray Absorption Near Edge Structure (XANES) spectrum was determined from the inflection point in the edge, i.e., the maximum in the first derivative of the XANES spectrum. The pre-edge energy was determined

from the maximum of the pre-edge peak. Experimental phase shift and back scattering amplitude were used to fit the extended X-ray absorption fine structure (EXAFS) data. V-O phase shift and back scattering amplitude were obtained from reference compound V(acac)₃ (6 V-O at 1.981 Å). Background removal and normalization procedures were carried out using the Athena software package using standard methods. Standard procedures based on WinXAS 3.2 software were used to extract the EXAFS data. The coordination parameters were obtained by a least square fit in R-space of the nearest neighbor, k²-weighted Fourier transform data.

1.5 High-Throughput Catalysis Screening

An automated synthesis platform – an Unchained Labs Inc. Core Module (CM3) - that is located in a custom-built N₂-filled glovebox (MB 200B, MBraun) in Argonne National Laboratory's High-throughput Research Facility, was used for high-throughput hydrogenation experiments. The CM3 is designed to perform solid and liquid handling as well as to process samples with on-deck heating, cooling, and stirring. Matrices of experiments and protocols were designed in Library Studio while Automation Studio (LEA software) was used for running the protocols. Simultaneous testing of all the catalysts and controls were carried out in multi-well plates that can hold 48 x 2 mL glass vials per run. In every catalysis run, a series of negative controls were implemented such as (1) the thermal sample, and (2) the metal-free silica. The solid catalysts were dispensed through disposable Shaker Vials (SV) with polytetrafluoroethylene (PTFE) hoppers and weighed using an automated balance (± 0.2 mg accuracy). 0.75 mL of a 0.25 M stock solution of diphenylacetylene in dodecane were used for the hydrogenation experiments. Each solution was dispensed using a Rainin dispense tool equipped with a disposable, 1-mL Positive Displacement Tip (PDT), operated by the CM3. The multi-well plate with vials was covered with a pin-hole Teflon gasket and a stainless steel pin-hole plate to ensure gas diffusion but to minimize cross-contamination between the vials. The multi-well plate was then transferred into a clam-shell reactor, which was sealed inside the glovebox. The clam-shell reactor was then taken out to the Screening Pressure Reactor (SPR, Unchained Labs Inc.), which is designed to carry out pressure reactions with heating and orbital shaking. The SPR system is controllable via software, so designed parameters including gas mixture, temperature ramp rate, soak temperature and soak time, shaking rate (rpm), target pressure and pressure limit are defined in the protocol before the experiment starts.

Initially, the SPR was flushed with 100 mL/min H₂, (UHP grade) for 15 min at room temperature, pressurized, and set to shake at 300 rpm. The reactor was then heated up slowly (1 °C/min ramp rate) to 75 °C. Under the given conditions, the pressure of the reactor reached 200 psi-g. After 20 h, the shaking was stopped, the reactor was cooled down to room temperature, and was flushed with 100 mL/min N₂ (UHP) for 15 min. The clam-shell reactor was then brought back to the glovebox. Aliquots were then transferred into filter vials (0.2 µm) to separate the solid catalysts from the organic solution and prevent the GC columns to be damaged.

For kinetic measurements, the Optimization Screening Reactor (OSR, Unchained Labs Inc.) located in the N₂-filled glovebox, was used. It has 8 parallel batch reactors with independent temperature and pressure control and a common overhead stirring. It also has the capability of sampling and injection during reaction. First, **1c** (456 mg for the diphenylacetylene run and 207 mg for the 1-octene run) was loaded manually. Then, 25 mL stock solution (0.25 M in dodecane) was added, also manually. The rest of the procedure was controlled by the LEA software; the reactors were purged with N₂ twice and then heated to 75 °C, flushed twice and pressurized with H₂ (UHP grade, oxygen and moisture trapped) up to 200 psi-g. Stirring was set at 300 rpm, but a settling delay was set at 15 s prior to sampling to avoid carrying over catalyst powder. Automated sampling of 100 µL was performed at various times, and dispensed into vials (Whatman Mini-UniPrep Syringeless Filter, 0.2 µm), on a 48 well plate, preloaded with 150 µL of dodecane and cooled at 5 °C to minimize evaporation while sitting on the deck.

1.5.1 GC-MS and GC-FID Analysis

The compositions of the reaction mixtures were determined using a Trace GC Ultra Gas Chromatograph system equipped with a Tri Plus RSH autosampler, an ISQ MS detector, and a FID (Thermo Scientific). The column used for the MS detector was an Agilent J&W DB-5 column (30 m × 0.25 mm × 0.25 µm film thickness) while the column used for the FID was an Agilent J&W DB-5MS column (30 m × 0.25 mm × 0.25µm film thickness). GC data were analyzed using the Thermo Xcalibur 2.2 SP1.48 software. The following method was used: a 0.5 µL split injection with a split ratio of 100 run under a constant gas flow of 1 mL/min. The oven temperature profile was as follows: initial temperature = 40 °C, hold for 0.5 minutes, ramp at 5 °C/min, final temperature = 200 °C.

1.5.2 Catalyst Recyclability and Leaching Tests

For the recyclability tests, 10 mg of catalyst **1c** was used with 0.75 mL of 0.25 M diphenylacetylene in dodecane. After the first reaction (75 °C, 200 psi-g H₂, 20 h), the supernatant was removed carefully and set aside for GC analyses. The “wet” catalyst was then rinsed with a fresh solution of diphenylacetylene in dodecane. This was repeated twice, before adding a fresh solution. For the leaching test, after the first reaction (75 °C, 200 psig H₂, 20 h), the supernatant was filtered and separated from the solid catalyst and used for a second reaction.

1.7 Micro-Reactor Activity Testing

Hydrogenation of ethylene was conducted using a fixed-bed flow reactor system equipped with Brooks 5850E mass flow controllers and a Thermcraft Model# LSP-1.63-0-6-1C-J9674/1A high-temperature furnace. A mixture containing 0.8% ethylene with a 1 to 2.3 ethylene-to-hydrogen ratio was first introduced to a homemade oxygen trap (Fe/SiO₂) in order to remove all the oxygen contained in the reactant mixture. The outlet stream of the oxygen trap was directed to 6 mm I.D. quartz reactor tube at a total flow rate of 20 mL/min. The catalyst bed was positioned at the center of the furnace, supported by quartz wool. The furnace temperature was altered by a Micromega[®] controller and was measured by a thermocouple located at the middle of the catalyst bed. The reaction was performed at 50 °C, 100 °C, 150 °C and 200 °C using catalyst amounts ranging from 50 mg to 200 mg. This resulted in bed heights of 2.5 to 3.5 cm (diluted with SiC). The exit of the reactor was connected to an Agilent/HP 6890 gas chromatograph (GC). Product identification and quantification were carried out using a FID (flame ionization detector). Calibration curves for ethylene and ethane were obtained prior to the experiment.

2. Results and Discussion

2.1 Synthesis of [(SiO₂)V(Mes)(THF)] (**1a-c**)

A 40 mL scintillation vial was charged with a slurry of 500 mg SiO_{2(200 °C)} in 15 mL toluene. A 5 mL toluene solution of [V(Mes)₃(THF)] (**1a** = 175 mg (0.37 mmol V); **1b** = 87 mg (0.18 mmol V); **1c** = 41.5 mg (0.09 mmol V)) was added drop-wise to the stirring slurry of SiO_{2(200 °C)} over 10 minutes. The dark blue reaction mixture decolorized within 10 to 30 minutes, the stirring stopped and the resulting dark purple solids filtered. The dark purple solids were then washed with two 5 mL portion of toluene and were dried under vacuum. The [(SiO₂)V(Mes)(THF)] products

were characterized by ICP-OES and combustion analysis to determine the %V, %C and %H loadings.

Table S1. Summary of elemental analysis results of catalysts **1a-c**.

Catalyst	V (%w/w)	Calculated		Found	
		C (% w/w)	H (% w/w)	C (% w/w)	H (% w/w)
1a	2.79	8.50	1.09	7.39	1.08
1b	1.25	3.80	0.49	4.42	0.64
1c	0.71	2.16	0.28	2.86	0.53

The above %C and %H composition of catalysts **1a** to **1c** are consistent with the presence of one mesitylene and a THF molecule per V center.

2.2 Synthesis of V_2O_5/SiO_2

Vanadia was installed onto SiO_2 surfaces via incipient wetness impregnation (IWI) following published methods.^{S9} A 10 mL aqueous solution of 1.2673 g anhydrous oxalic acid ($H_2C_2O_4$) was mixed with a 10-mL aqueous solution of 0.7892 g ammonium metavanadate (NH_4VO_3), and the resulting mixture heated to 60 °C. Silica (10.3725 g SiO_2) was then added to create a slurry which was stirred overnight. The resulting dark teal blue solids were dried for 24 h at 110 °C. After drying, the brown-gray solids were calcined in air at 500 °C for 11 h to give a bright ochre yellow powder (2.37 wt% V). Characterization via TEM imaging indicated the presence of tiny aggregates (<2 nm diameter) relatively uniformly dispersed throughout the support.

2.3 Synthesis of $[(SiO_2)V(Mes)(THF)]-2,2'$ -bipyridine derivatives (**2a-c**)

Catalyst **1a** was purposefully poisoned with various loadings of 2,2'-bipyridine: (**2a**) 25%, (**2b**) 50%, and (**2c**) 100% of all V sites. The following methodology was employed in the synthesis of derivatives **2a-c**: A 20 mL scintillation vial was charged with a slurry of 200 mg **1a** (0.11 mmol V) was prepared in 5 mL toluene. A 3 mL toluene solution of 2,2'-bipyridine (**2a** = 4.3 mg (0.27 mmol V); **2b** = 8.6 mg (0.56 mmol V); **2c** = 17.1 mg (0.11 mmol)) was added drop-wise to the stirring slurry of **1a** over 10 minutes. The reaction mixture was stirred for 1 h, the stirring stopped and the resulting darker solids filtered. The solids were then washed with two 5 mL portion of toluene and were dried *in vacuo*.

2.4 NMR-scale vanadation of SiO_2 with $[V(Mes)_3(THF)]$

$[V(Mes)_3(THF)]$ (11.2 mg, 0.0235 mmol), SiO_2 (110 mg), and 1,3,5-tritertbutyl benzene (5.8 mg, 0.024 mmol; internal standard) were added to a 4 mL vial containing a stir bar. C_6D_6 (1 mL)

was then added and the slurry was allowed to stir for 1 h during which time the white silica turned dark-purple. The slurry was allowed to settle and the colorless supernatant was filtered into an NMR tube for analysis. Comparison of the ^1H NMR peak areas for mesitylene and 1,3,5-tritertbutyl benzene revealed that 0.050 mmol of mesitylene were liberated, corresponding to 2.1 mol mesitylene per mol of $[\text{V}(\text{Mes})_3(\text{THF})]$ precursor. This procedure was repeated twice (average mol of mesitylene per mol of $[\text{V}(\text{Mes})_3(\text{THF})]$ released: 2.03 mol).

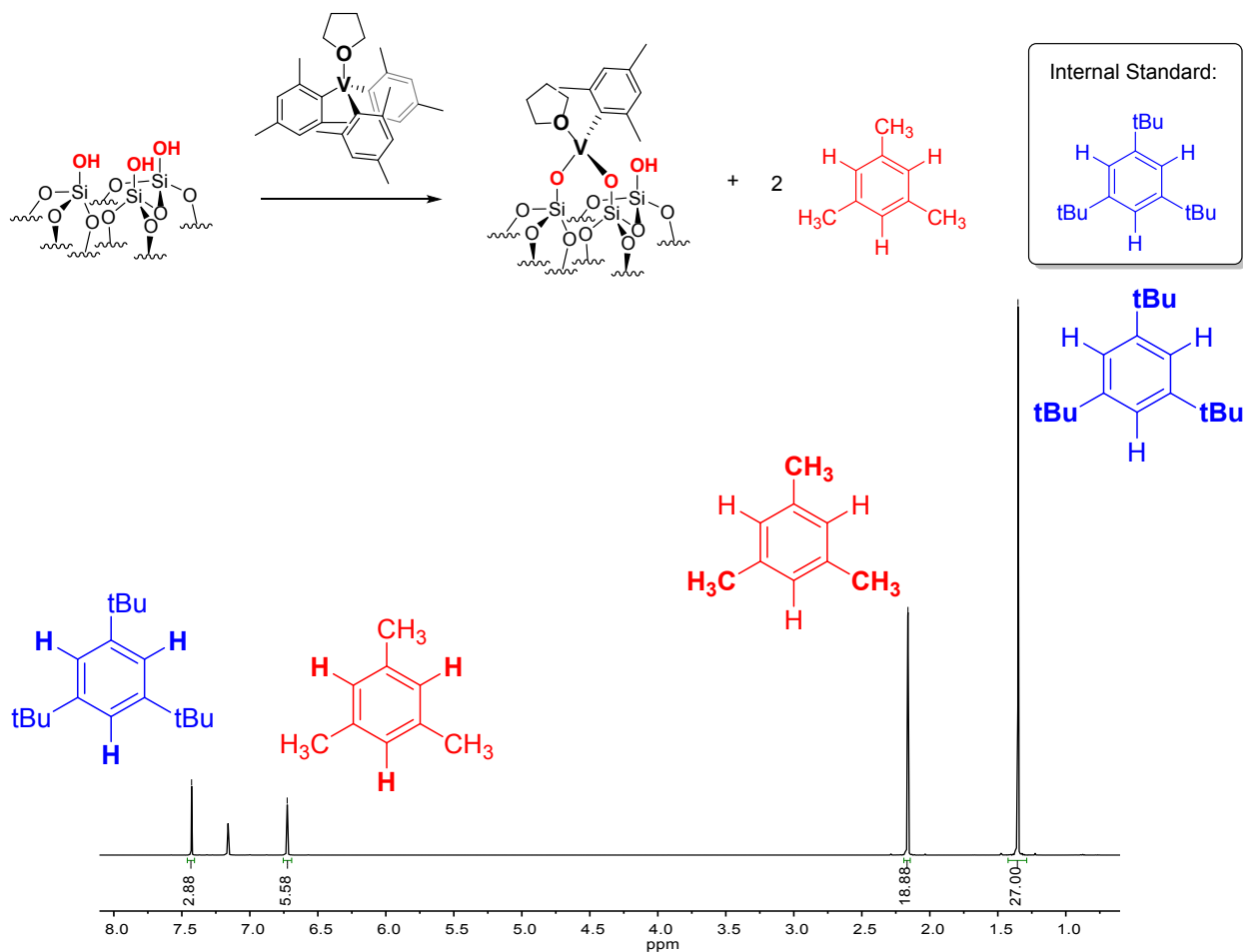


Figure S1. NMR-scale vanadation of $\text{SiO}_2(200^\circ\text{C})$ in C_6D_6 in the presence of 1,3,5-*tert*-butylbenzene (internal standard).

2.5 TGA-MS

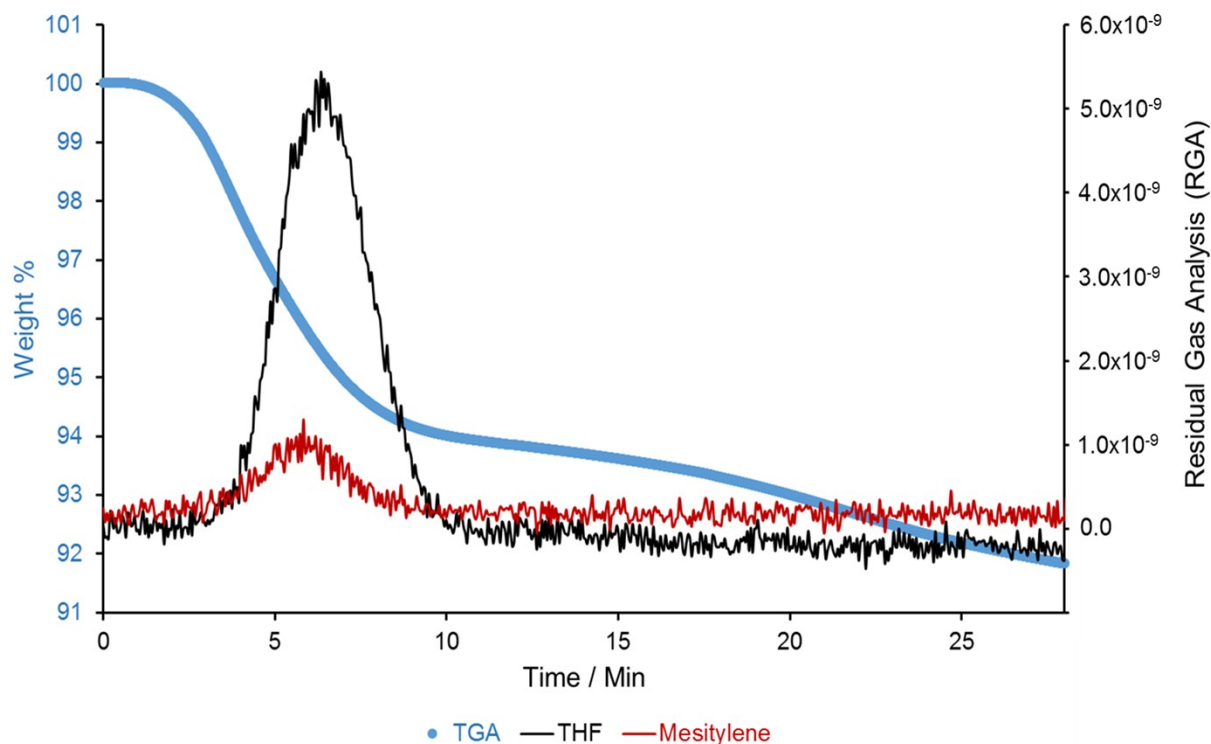


Figure S2. TGA-MS analysis of **1**. The area under the Mesitylene curve in the MS is lower than that of THF. This may be due to partial condensation in the capillary tube between the TGA and the mass analyzer. However, the mass loss (TGA, ~6.5% m/m) indicates the presence of one THF molecule and one mesityl ligand per vanadium. Our proposed structure for $[(\text{SiO}_2)\text{V}(\text{Mes})(\text{THF})]$ is supplemented with findings from other characterization results (i.e., combustion analysis, solution-phase ^1H NMR).

2.6 EPR Spectroscopy

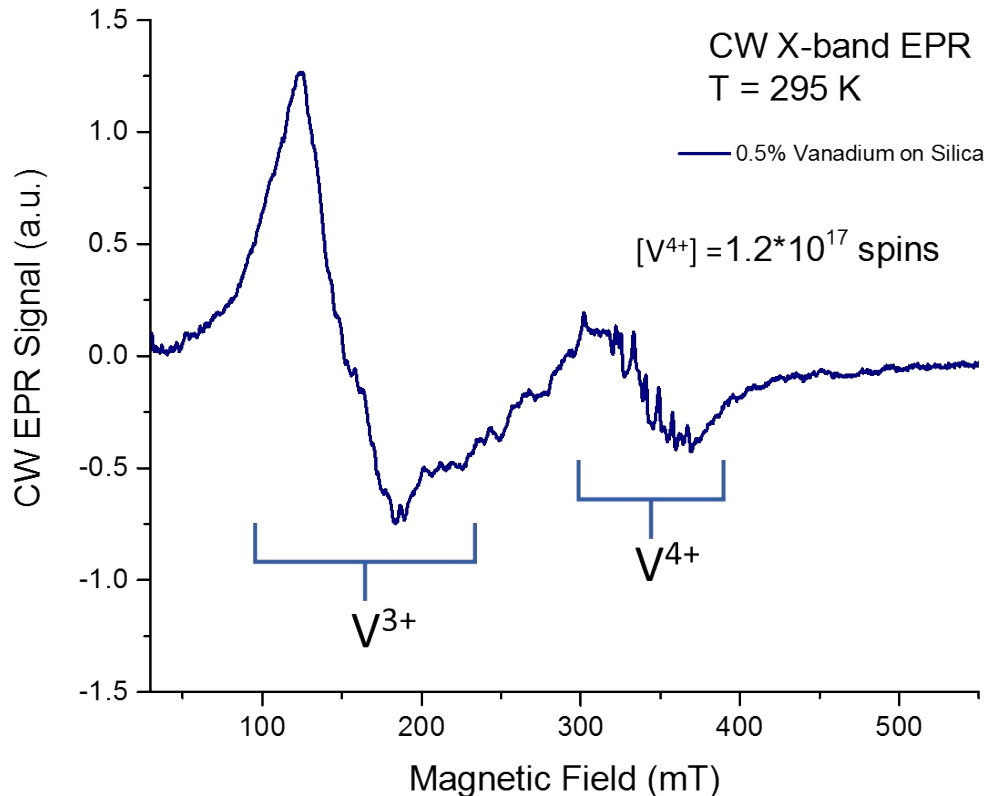


Figure S3. Room-temperature, continuous wave (cw) EPR spectrum at X-band of **1b**. The spectrum consists of two broad signals, one in the $g = 2$ region, centered at 330 mT, and another one in $g \approx 4$ region, centered at 160 mT.

Lines around $g \approx 2$ were assigned to V⁴⁺. This vanadium ion has only one unpaired electron spin ($S = 1/2$) and exhibits a characteristic multiline, broad (approximately 100 mT) EPR spectrum.^{S10} In contrast, V³⁺ has two unpaired electrons and is a high spin state with $S = 1$. This type of vanadium ion typically demonstrate a large zero-field splitting, often ca. 8 cm⁻¹, and thus cannot be completely characterized by conventional EPR spectroscopy with a microwave energy of 0.3 cm⁻¹ at X-band. However, EPR of V³⁺ exhibits forbidden transitions of the type $\Delta M_S = 2$ at half resonance field, $g \approx 4$. This transition is seen as a very strong signal in $g \approx 4$ region. Quantification of the spins reveals that the relative concentration of V⁴⁺ in the sample is <1% of the total vanadium concentration.

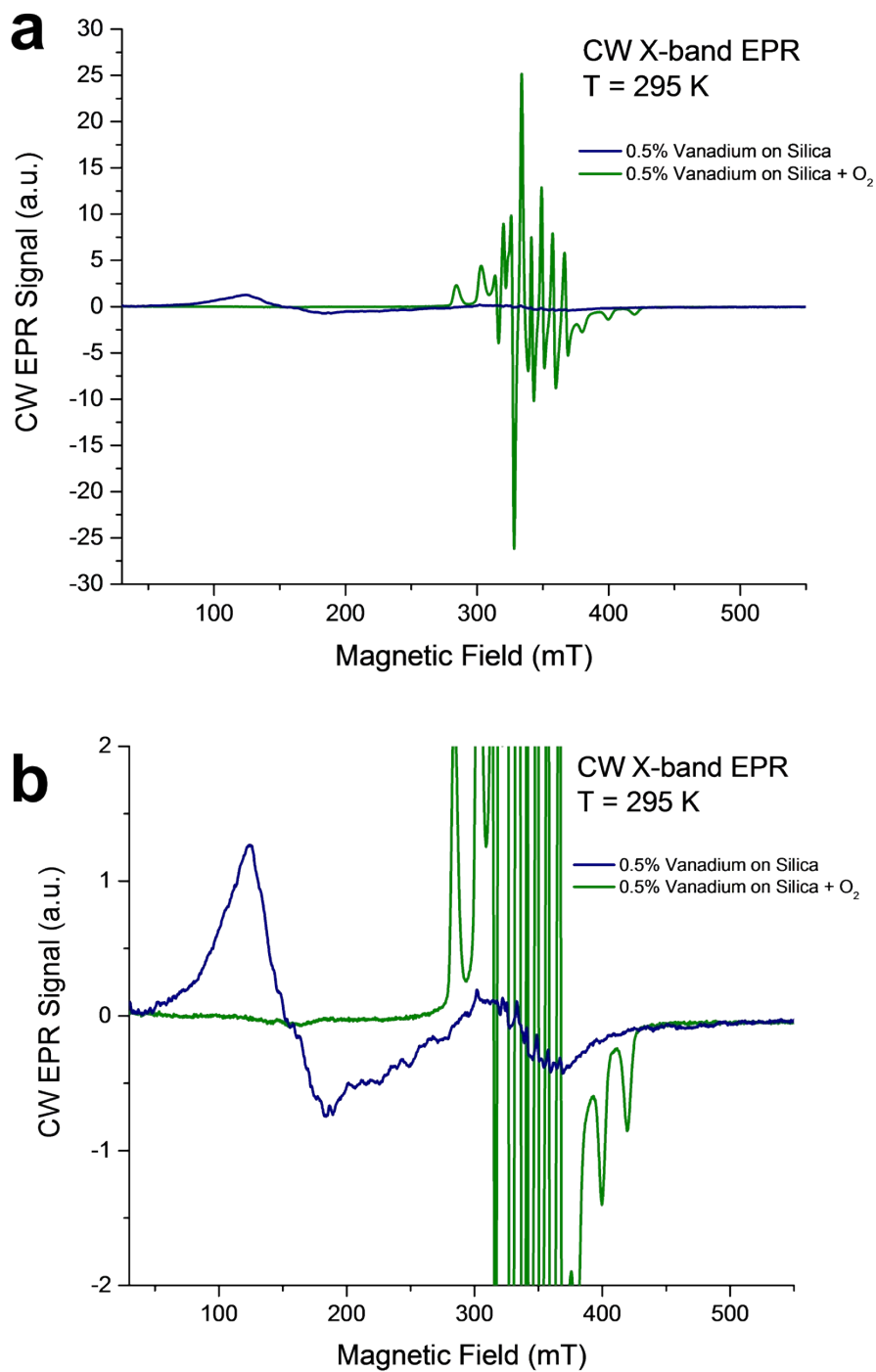


Figure S4. Room-temperature, continuous-wave (cw) EPR spectrum at X-band of **1b** after exposition to air. This procedure is expected to oxidize V³⁺ further to V⁴⁺. Indeed, the EPR spectrum recorded after oxidation shows a very intense V⁴⁺ signal, which is a typical spectrum for vanadyl (IV) ion with oxygen coordination,^{S10} and absence of the V³⁺ signal at $g \approx 4$.

2.7 XPS Analysis Results

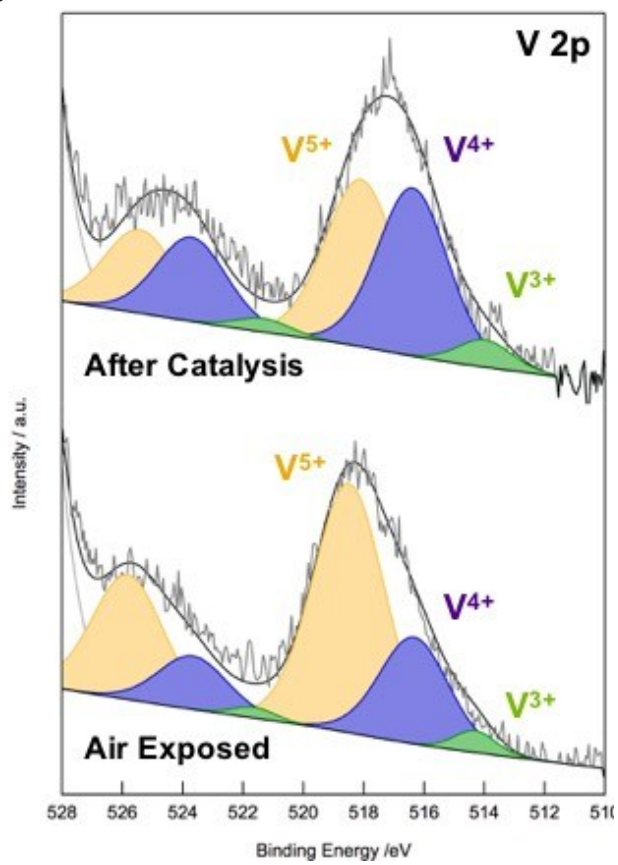


Figure S5. XPS analysis of air-exposed **1a**.

2.8 DRUV-Vis Spectroscopy

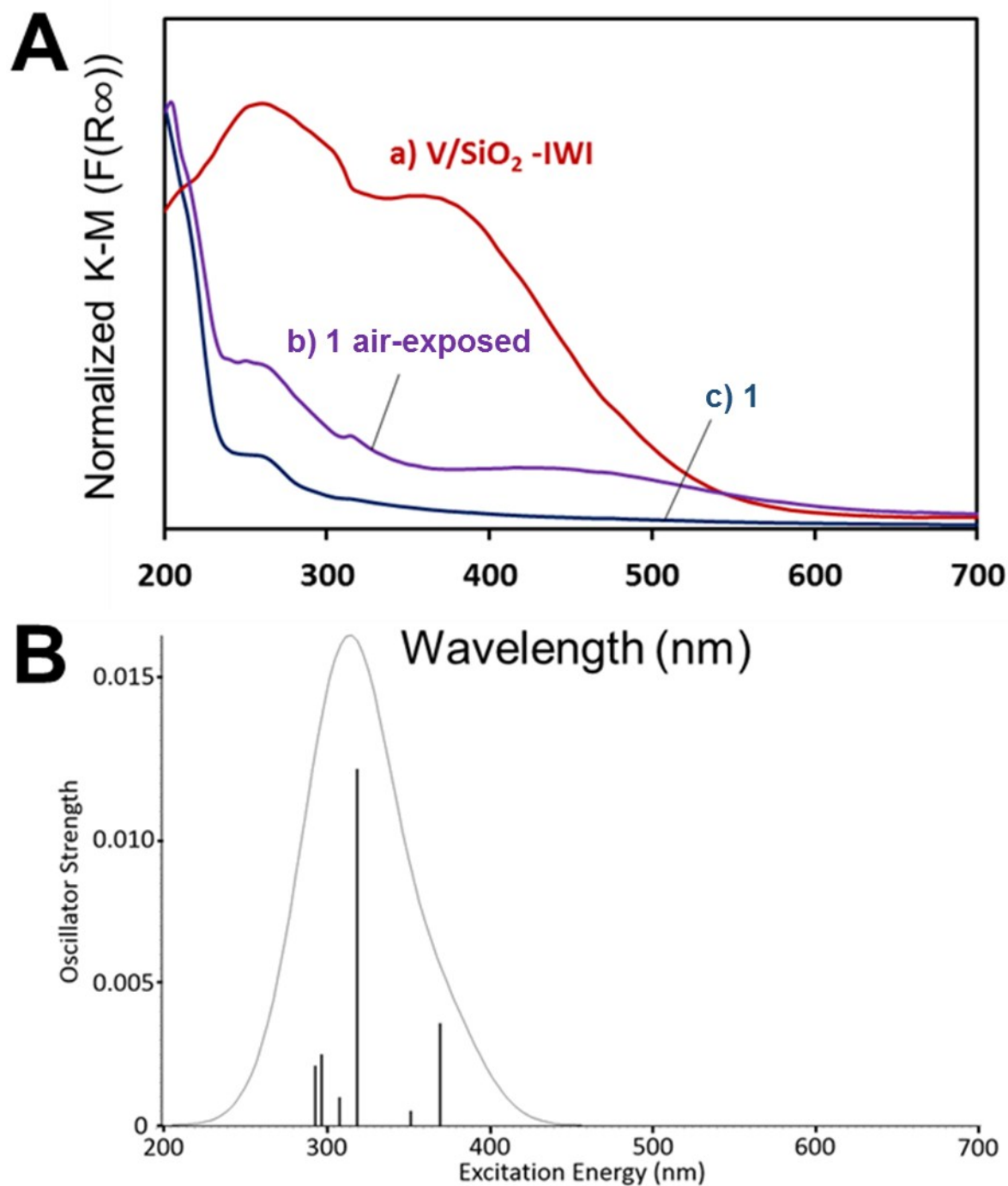


Figure S6. DRUV-Vis spectra of supported V systems: (A) experimental UV-Vis spectra of (a) V₂O₅/SiO₂ (red), (b) **1** air-exposed (purple), and (c) **1**; (B) DFT-simulated UV-Vis spectrum of **1**.

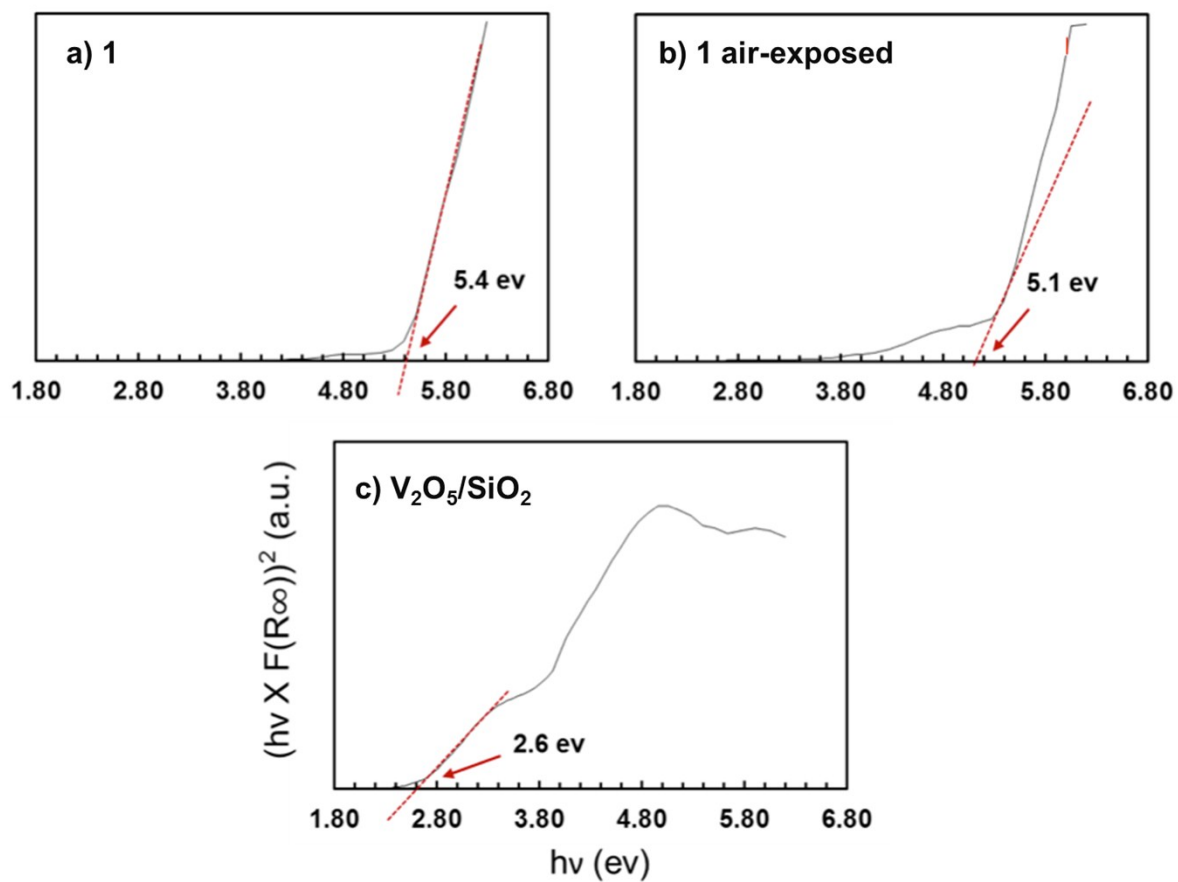


Figure S7. DRUV-Vis absorption edge energies of (a) **1**, (b) **1** air-exposed, and (c) V_2O_5/SiO_2 .

2.9 DFT Calculations

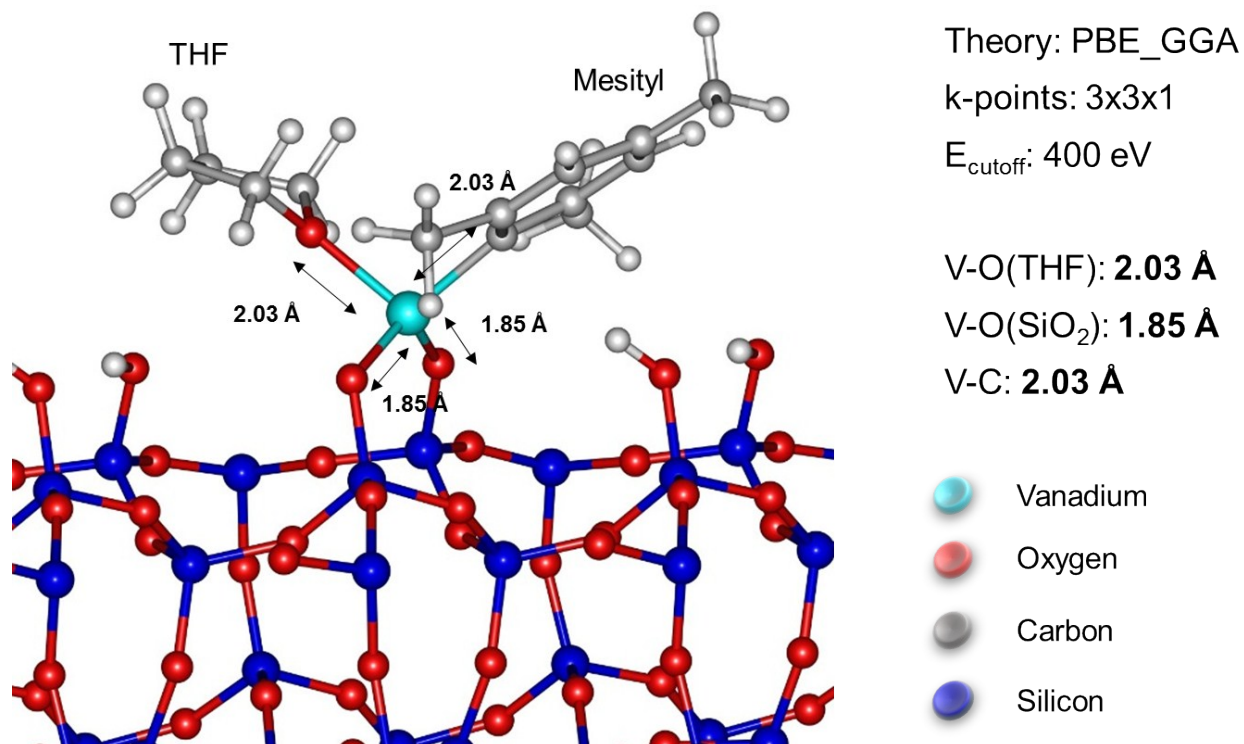
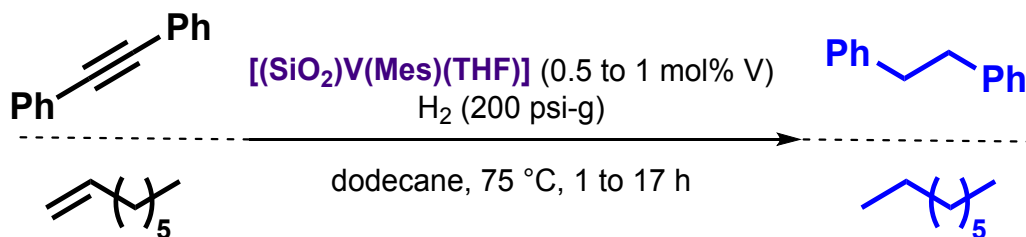


Figure S8. Structure of the V³⁺ sites in **1** based on periodic DFT calculations.

2.10 SPR Catalyst Testing and Catalyst Recyclability Results

Table S2. Comparison of hydrogenation activity of catalysts **1a-c** with [(CatPOP)V(Mes)(THF)].



Sample	mol % V	Conversion	Selectivity to Stilbenes	TOF (h ⁻¹)
0.71% 1a	0.5	88.0	89.9	10
1.25% 1b	0.4	90.5	85.9	13.6
2.79% 1c	0.5	91.3	78.3	10.6
5.73% [(CatPOP)V(Mes)(THF)]	0.5	25.5	91.4	2.8

Comparison of diphenylacetylene hydrogenation experiments between the [(CatPOP)V(Mes)(THF)] reference and [(SiO₂)V(Mes)(THF)] catalysts at three different V loadings: (**1a**) 0.71% V (w/w), (**1b**) 1.25% and (**1c**) 2.79%. The rationale for employing three different V loadings on SiO₂ was also to look at the effects of V surface concentrations on SiO₂. All four hydrogenation experiments in Table S2 were carried out at identical V loading (0.5 mol% V; 0.25M diphenylacetylene). The similar conversions observed from the three [(SiO₂)V(Mes)(THF)] catalysts validates the single-site nature of the material; that an identical number of sites/V loading is responsible for the catalytic activity, regardless of V dispersion on the SiO₂ surface.

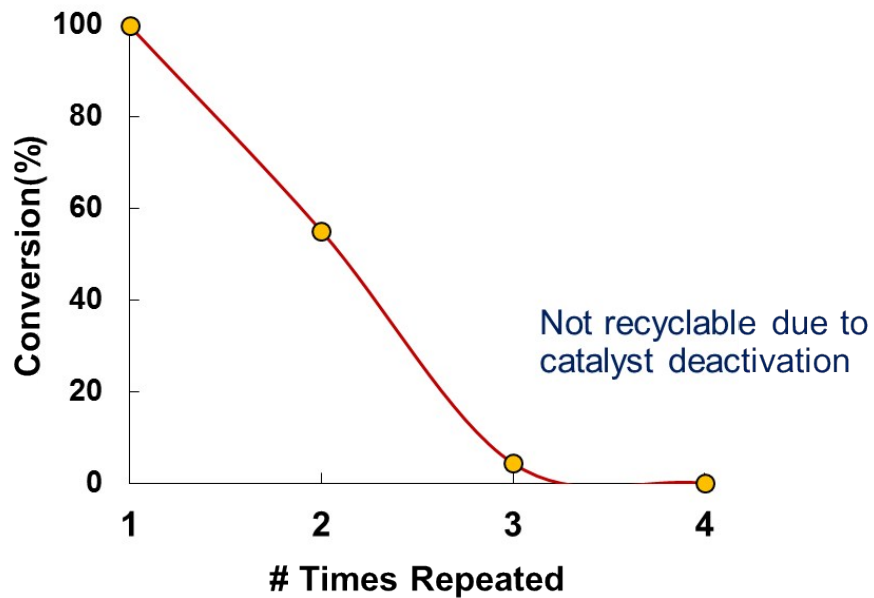


Figure S9. Recyclability test of **1** for solution-phase hydrogenation of diphenylacetylene using 0.75 mL of 0.25M diphenylacetylene in dodecane (75 °C, 200 psi-g H₂, 20 h for each reaction).

2.11 TEM Imaging

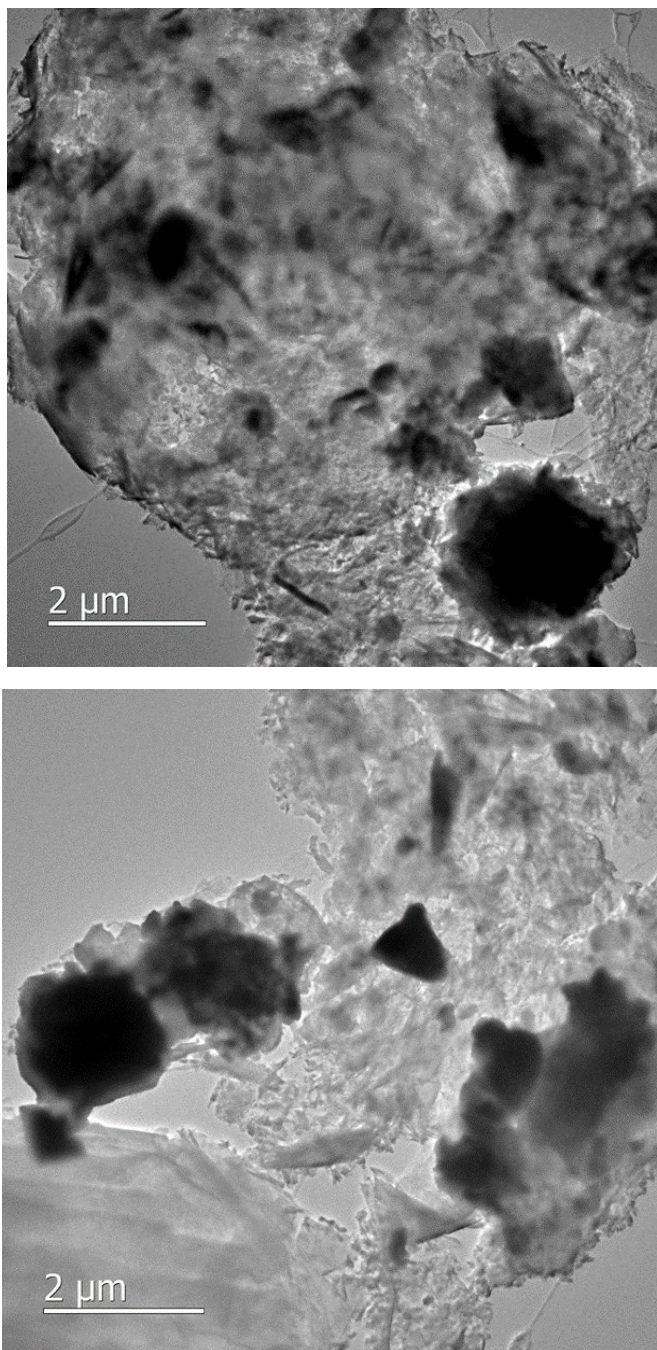


Figure S10. TEM imaging of catalyst **1** showing the formation of agglomerated V species after solution-phase hydrogenation of diphenylacetylene.

2.12. UV Raman Results

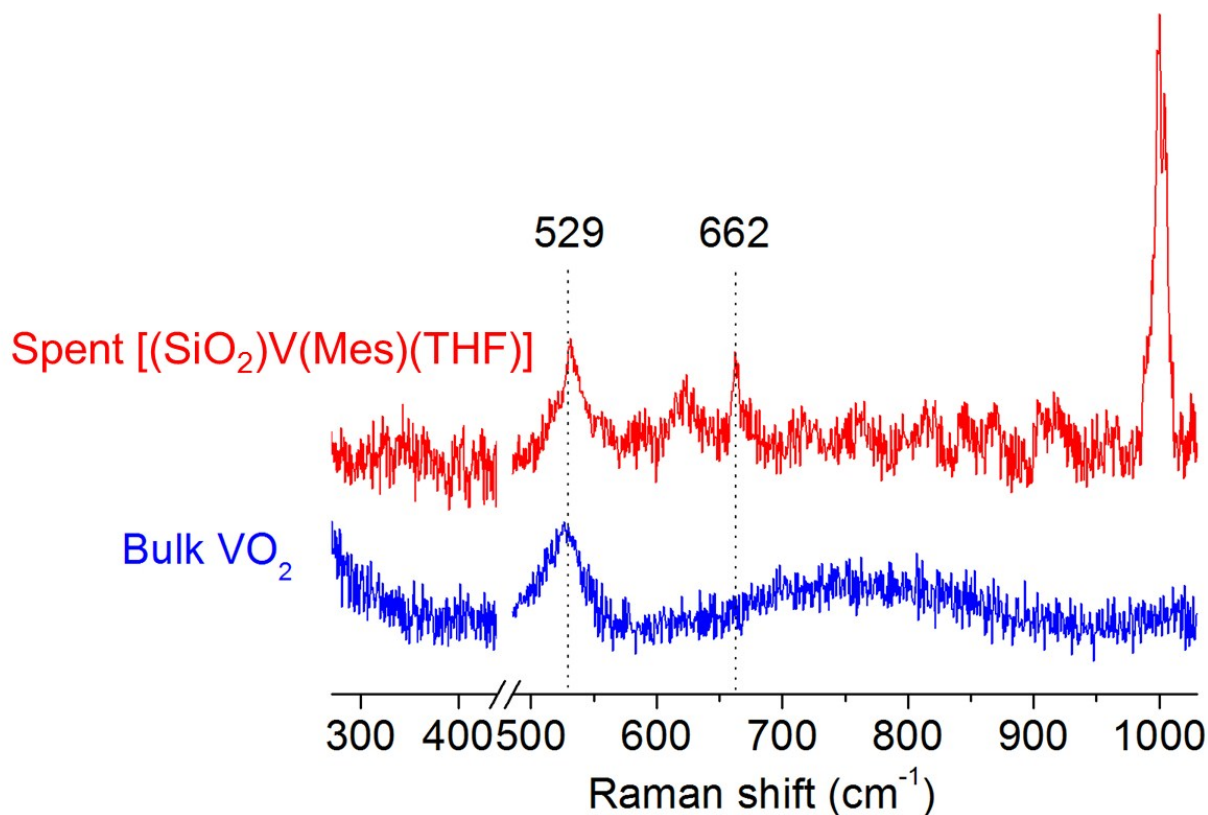


Figure S11. A comparison of the UV Raman spectra of spent **1** and bulk VO₂.

UV Raman spectrum of spent **1** shows a notable band at 529 cm^{-1} which matches well with the characteristic UV Raman band of bulk VO₂ (Fig. S11) suggesting the presence of VO₂. This result is in good agreement with the finding of V⁴⁺ signal by EPR (Figs. S3 and S4). And, a Raman band appearing at 662 cm^{-1} of the spent **1** can be assigned to asymmetric V-O-V stretching vibration, which typically appears in the 630-780 cm^{-1} region.^{S11, 12} The presence of V-O-V vibrations indicates the existence of oligomeric/polymeric VO_x species in spent VO_x catalyst, which is consistent with the finding of agglomerated particles by TEM (Fig. S10).

2.13 Variable-Temperature Gas-Phase Hydrogenation of Ethylene with Catalyst 1.

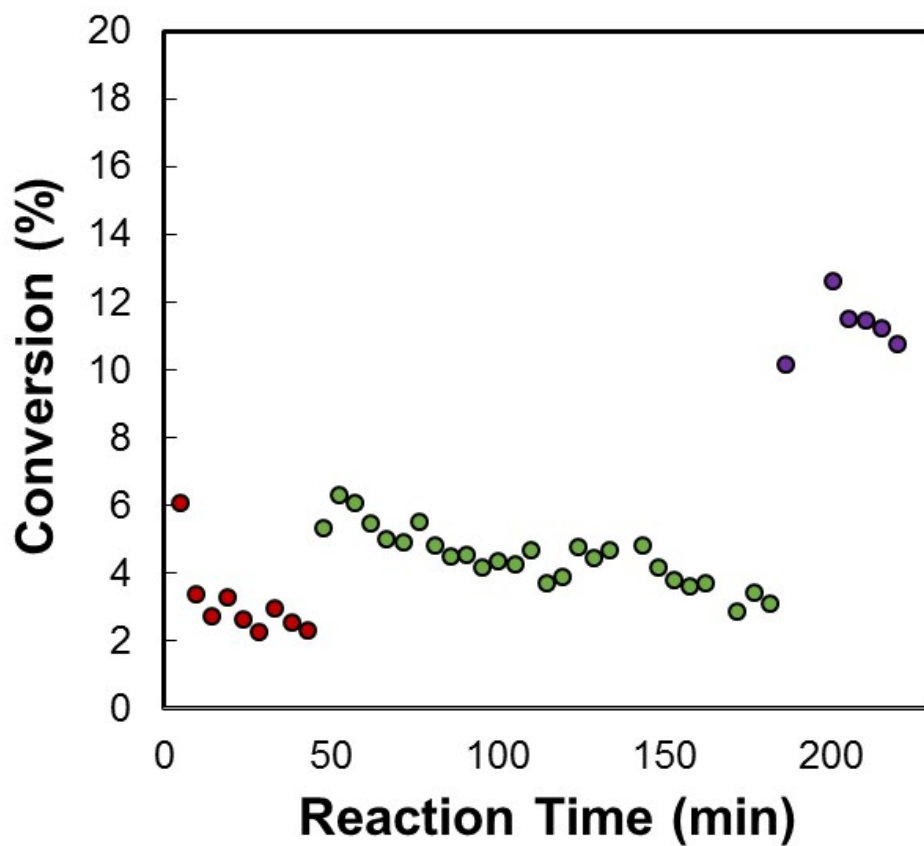


Figure S12. Gas-phase hydrogenation of ethylene at different temperatures: 25 °C (red), 50 °C (green) and 100 °C (purple).

3. References

- S1. M. Vivanco, J. Ruiz, C. Floriani, A. Chiesi-Villa and C. Rizzoli, *Organometallics*, 1993, **12**, 1794-1801.
2. H. Kim, K. M. Kosuda, R. P. Van Duyne and P. C. Stair, *Chem. Soc. Rev.*, 2010, **39**, 4820-4844.
3. U. Das, G. Zhang, B. Hu, A. S. Hock, P. C. Redfern, J. T. Miller and L. A. Curtiss, *Acs Catal*, 2015, **5**, 7177-7185.
4. G. Kresse and J. Hafner, *Physical Review B*, 1993, **47**, 558-561.
5. G. Kresse and J. Hafner, *Physical Review B*, 1994, **49**, 14251-14269.
6. G. Kresse and J. Furthmüller, *Physical Review B*, 1996, **54**, 11169-11186.
7. G. Kresse and J. Furthmüller, *Computational Materials Science*, 1996, **6**, 15-50.
8. Gaussian 09, Revision A.02, M. J. Frisch, G. W. Trucks, H. B. Schlegel, G. E. Scuseria, M. A. Robb, J. R. Cheeseman, G. Scalmani, V. Barone, G. A. Petersson, H. Nakatsuji, X. Li, M. Caricato, A. Marenich, J. Bloino, B. G. Janesko, R. Gomperts, B. Mennucci, H. P. Hratchian, J. V. Ortiz, A. F. Izmaylov, J. L. Sonnenberg, D. Williams-Young, F. Ding, F. Lipparini, F. Egidi, J. Goings, B. Peng, A. Petrone, T. Henderson, D. Ranasinghe, V. G. Zakrzewski, J. Gao, N. Rega, G. Zheng, W. Liang, M. Hada, M. Ehara, K. Toyota, R. Fukuda, J. Hasegawa, M. Ishida, T. Nakajima, Y. Honda, O. Kitao, H. Nakai, T. Vreven, K. Throssell, J. A. Montgomery, Jr., J. E. Peralta, F. Ogliaro, M. Bearpark, J. J. Heyd, E. Brothers, K. N. Kudin, V. N. Staroverov, T. Keith, R. Kobayashi, J. Normand, K. Raghavachari, A. Rendell, J. C. Burant, S. S. Iyengar, J. Tomasi, M. Cossi, J. M. Millam, M. Klene, C. Adamo, R. Cammi, J. W. Ochterski, R. L. Martin, K. Morokuma, O. Farkas, J. B. Foresman, and D. J. Fox, Gaussian, Inc., Wallingford CT, 2016.
9. S. Barman, N. Maity, K. Bhatte, S. Ould-Chikh, O. Dachwald, C. Haeßner, Y. Saih, E. Abou-Hamad, I. Llorens, J.-L. Hazemann, K. Köhler, V. D' Elia and J.-M. Basset, *ACS Catal.*, 2016, **6**, 5908-5921.
10. D. Sanna, G. Sciortino, V. Ugone, G. Micera and E. Garrriba, *Inorg. Chem.*, 2016, **55**, 7373-7387.
11. R. G. Brown and S. D. Ross, *Spectrochimica Acta A: Mol. Spec.*, 1972, **28**, 1263-1274.
12. Y. S. Park and H. F. Shurvell, *J. Raman Spectrosc.*, 1989, **20**, 673-681.